IOSR Journal of Applied Physics (IOSR-JAP)
e-ISSN: 2278-4861.Volume 7, Issue 2 Ver. II (Mar. - Apr. 2015), PP 08-15
www.iosrjournals.org

Efficiency Improvement of p-i-n Structure over p-n Structure and Effect of p-Layer and i-Layer Properties on Electrical Measurements of Gallium Nitride and Indium Nitride Alloy Based Thin Film Solar Cell Using AMPS - 1D

A. K. Das
Department of Physics, P. K. College, Contai; Contai-721401, India.

Abstract: *The effect of p-layer and i-layer characteristics such as doping concentration and thickness on the electrical behaviors of the p-n and p-i-n GaInN solar cells such as electric field, photo generation rate and recombination rate through the cells are studied. Introducing i (un-doped) layer between p and n-doped layers to form the p-i-n solar cell is an effective approach in improving performances with respect to p-n cell. The efficiency improvement of 3.0 % of p-i-n cell over p-n cell is observed for low doping concentration ($< 5 \times 10^{16}\ cm^{-3}$) and high surface recombination ($10^7 cm/s$) of less passivated p-layer surface of the device. The photo-generated short-circuit current density (J_{sc}) and the open-circuit voltage (V_{oc}) of both structures under AM 1.5G (one sun) illumination (1kW/m^2, 0.32 – 0.88 µm) of photon flux from ASTM G173-03 are simulated for different p-layer doping concentrations varying from 5×10^{16} to $1 \times 10^{20}\ cm^{-3}$.*

Keywords: *AMPS-1D simulation, electric field, efficiency, photo-generation and recombination, GaInN thin film, solar cell.*

I. Introduction

Solar cells are the most effective alternative energy source which may be one of the conventional power sources. To minimize CO_2 emission from fossil fuel, alternative forms of power production have been continuing effectively since last seven decades using solar energy which is plentiful, clean, free of cost, easily available and non toxic that can be used in photo voltaic cell which converts directly from sunlight into electricity. Various type of solar cell structures have been developed by different technologies in which them, the thin film technology is most powerful for large area production. Alloy of gallium nitride (GaN) and indium nitride (InN) has high absorption co-efficient and hence the high efficiency than usually used silicon or silicon-germanium alloy based thin film solar cell. Also GaInN alloy has high thermal conductivity, high carrier drift velocity and high radiation resistance those properties are suitable for use in extreme weather condition of environments.

The electrical properties such as electric field, photo-generation and recombination through p-n and p-i-n cells depend on p-layer properties such as doping (acceptor) concentration, surface recombination, and thickness of p-layer and i-layer those are key parameters for designing thin film photovoltaic cell.

Jani et al. [1] designed low In content $Ga_{1-x}In_xN$ (x = 0.04 ~ 0.05) p-i-n and quantum well solar cells and characterized them. Xiaobin Zang et al [2] reported the optimum efficiency (20.284%) of single junction solar cells of 65% In content using AMPS-1D. Hamzaoui et al [3] analyzed GaInN solar cells with up to six junctions getting preliminary results concerning the relationship of open circuit voltage and short-circuit current density variation with the junction numbers. Tae Hoon Seo et al [4] have recently fabricated low In (15%) content $Ga_{0.85}In_{0.15}N$ -based multiple quantum well (MQW) solar cell as absorbing layer between p-GaN and n-GaN of band gap of 3.40 eV and improved photovoltaic effects using graphene network on indium tin oxide (ITO) nanodot as anti-reflecting coating (ARC) on p-GaN epilayer. However, the fabrication of high In content GaInN solar cell is now challenging.

II. Simulation Model

Modeling of the device is based on the simultaneous solution of transport equations such as Poisson's equations, continuity equations and current density equations for holes and electrons [5] using finite differences and Newton-Rapshon method in AMPS-1D (Analysis of Microelectronic and Photonic Structures in one dimension) to estimate the steady state band diagram, generation and recombination profile as well as carrier transport in p-n and p-i-n structures of the solar cells. The external most important parameters of a solar cell are short-circuit current, the open circuit voltage, fill factor and efficiency. The short-circuit current is due to the generation and collection of photo-generated carriers. Thus, ideally, it is equal to photo-generated current which is the largest current that can flow through the solar cell.

In one dimension, Poisson's equation can be written as

$$\frac{d}{dX}\left(-\varepsilon(X)\frac{d\Psi}{dX}\right) = q * [p(X) - n(X) + N_D^+(X) - N_A^-(X) + p_t(X) - n_t(X)] \quad (1)$$

where the electrostatic potential Ψ, the free electron n , free hole p , trapped electron n_t, and trapped hole p_t as well as the ionized donor-like doping N_D^+ and ionized acceptor-like doping N_A^- concentrations are all functions of the position co-ordinate X. Here, ε is the permittivity and q is the magnitude of charge of an electron. The continuity equations for the free electrons and holes in the delocalized (band) states of the conduction band and valence band, respectively, have the forms:

for electron $$\frac{1}{q}\left(\frac{dJ_n}{dX}\right) = -G_{op}(X) + R(X) \quad (2)$$

and for hole $$\frac{1}{q}\left(\frac{dJ_p}{dX}\right) = G_{op}(X) - R(X) \quad (3)$$

where J_n and J_p are, respectively, the electron and hole current densities. The term R(X) is the net recombination rate resulting from direct band-to-band recombination and indirect Shockley-Read-Hall (SRH) recombination through gap (localized) states and the term $G_{op}(X)$ is the optical generation rate as a function of X due to externally imposed illumination.

III. Modeling Parameters

Band gap (E_g) [6]: The direct band gap $Ga_{1-x}In_xN$ material can be tuned from energy gap 3.4 eV of GaN to 0.7 eV of InN as a function of x by the following relation

$$E_g(x) = (1-x)E_{g\,GaN} + xE_{g\,InN} - \beta(1-x) \quad (4)$$

where $E_{g\,GaN}$ and $E_{g\,InN}$ are, respectively, the energy gap for GaN and InN materials, x is the In mole fraction, and $\beta = 1.43$ eV be the bending factor.

Absorption coefficient (α) [2]**:** Efficiency of solar cell depends on some factors including absorption coefficient that plays a significant role as a function of energies of incident photons and band gap of GaInN.

$$\alpha(\mu m^{-1}) = A\sqrt{\frac{1.2398}{\lambda} - E_g} \quad (5)$$

where λ be the wave length of incident photon in μm and A be the average weighing factor of the absorption coefficient which is $2.2 \times 10^5\ \mu m^{-1}(eV)^{-\frac{1}{2}}$. Also other parametric equations as a function of E_g and hence in x are given by

Electron affinity (χ) [2, 7] **:** in eV $$\chi(E_g) = \chi_{GaN} + 0.7(E_{g\,GaN} - E_g) \quad (6)$$

where $\chi_{GaN} = 4.1$ be the electron affinity of GaN.

Relative permittivity (ε_r)[7]: The relative permittivity or dielectric constant is a measure of optical properties of GaInN alloy layers and is given by the following relation as a function of x

$$\varepsilon_r(x) = (1-x)\varepsilon_{GaN} + \varepsilon_{InN}\,x \quad * \quad (7)$$

where $\varepsilon_{GaN} = 10.4$ and $\varepsilon_{InN} = 14.6$ be the dielectric constants of GaN and InN, respectively.

Effective density of states (N_C, N_V) [7]**:** The electron and hole concentration in conduction and valence band in a semiconductor can be written, respectively, as

$$n = N_C e^{\frac{(E_f - E_c)}{kT}}, \text{ and } \quad p = N_V e^{\frac{(E_v - E_f)}{kT}} \quad (8)$$

where N_C , E_c and N_V , E_v are the effective density of states and mobility edges in the conduction and valence band, respectively. E_f be the Fermi level at absolute temperature T and k is Boltzmann constant. Effective density of states in the conduction and valence bands, respectively,

$$N_c(x) = (1-x)N_{c\,GaN} + xN_{c\,InN} \quad * \tag{9}$$

and $$N_v(x) = (1-x)N_{v\,GaN} + xN_{v\,InN} \quad * \tag{10}$$

where $N_{c\,GaN} = 2.3 \times 10^{18}\ cm^{-3}$, $N_{c\,InN} = 9.0 \times 10^{17}\ cm^{-3}$; $N_{v\,GaN} = 1.8 \times 10^{19}\ cm^{-3}$ and $N_{v\,InN} = 5.3 \times 10^{19}\ cm^{-3}$ are the effective density of states in conduction and valence band of GaN and InN, respectively.

Electron mobility (μ_n) [8]**:** in cm^2/volt-s $$\mu_n(N_z) = \mu_{min,n} + \frac{\mu_{max,n} - \mu_{min,n}}{1+(\frac{N_z}{N_{g,n}})^{\gamma n}} \tag{11}$$

Hole mobility (μ_p) [8]**:** in cm^2/volt-s $$\mu_p(N_z) = \mu_{min,p} + \frac{\mu_{max,p} - \mu_{min,p}}{1+(\frac{N_z}{N_{g,p}})^{\gamma p}} \tag{12}$$

The electron and hole mobility of GaInN is assumed similar to GaN, where N_z be the doping concentration such as for z = A,D denotes the acceptor and donor concentration of p and n-layers, respectively and the other model parameters $\mu_{max,n}$, $\mu_{max,p}$; $\mu_{min,n}$, $\mu_{min,p}$; $\mathcal{N}_{g,n}$, $\mathcal{N}_{g,p}$ and γ_n, γ_p depend on the type of semiconductor [8] which are given by in the following Table 1.

Table 1 Model parameters used in the calculation of the mobility of electron and hole

Type of carriers	Parameters			
	$\mu_{max,i}(cm^2V^{-1}s^{-1})$	$\mu_{min,i}(cm^2V^{-1}s^{-1})$	$N_{g,i}(cm^{-3})$	γ_i
Electron $(i=n)$	10^3	55	2×10^{17}	1
Hole $(i=p)$	170	3	3×10^{17}	2

The above * marked equations are obtained from the linear approximation of the corresponding parameters of GaN and InN.

IV. Cell Structures

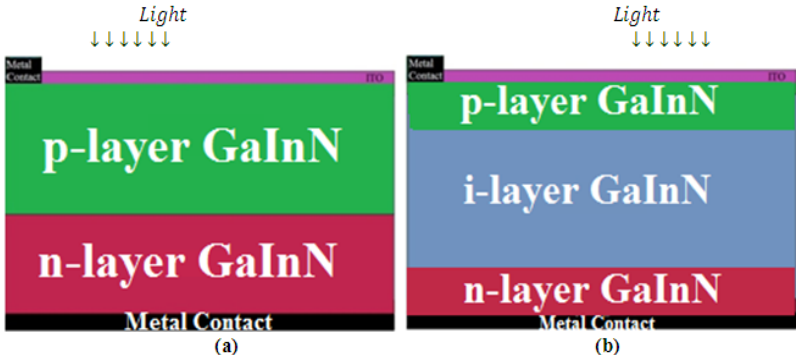

Figure 1: Schematic diagram of **(a)** p-n and **(b)** p-i-n solar cells of total device thickness 290 nm.

V. Solar Cell Parameters

Table 2: Model parameters used in the simulation for p-n and p-i-n cells

Solar Cells / Parameters	p-n		p-i-n		
	p-layer	n-layer	p-layer	i-layer	n-layer
Thickness (nm)	200	90	10	270	10
Dielectric constant	12.98	12.98	12.64	12.98	12.64
Energy gap (eV)	1.40	1.40	1.60	1.40	1.60
Mobility of electron (cm^2/V-s)	325.0	325.0	811.0	1000.0	325.0
Mobility of hole (cm^2/V-s)	47.2059	47.2059	165.48648	170.0	47.2059
Acceptor /Donor concentration (cm^{-3})	5.0×10^{17}/ --	-- /5.0×10^{17}	5.0×10^{16}/ --	--	-- /5.0×10^{17}
Effective density of states in					
(i) conduction band, N_c (cm^{-3})	1.44×10^{18}	1.44×10^{18}	1.55×10^{18}	1.44×10^{18}	1.55×10^{18}
(ii) valence band, N_v (cm^{-3})	3.95×10^{19}	3.95×10^{19}	3.67×10^{19}	3.95×10^{19}	3.67×10^{19}
Electron affinity (eV)	5.5	5.5	5.36	5.5	5.36

V. Results And Discussions

The electrical behaviors of p-layer for p-n and p-i-n cells (fig. 1) and i-layer for later cell are studied for In concentration of 62% of first cell including i-layer of later cell and 53.5% for top and bottom layers of p-i-n cell so that the total device thickness remains constant at 290 nm in order to obtain the optimum efficiency by varying p-layer properties such as doping concentration and thickness of the cells. The variations of the electrical properties inside the solar cell such as the electric field intensity (**E**), the distribution of photo generation (G_{op}) and recombination (R) with variation of p-layer properties are studied. The electric field intensity at the p/n and p/i interfaces for the p-n and p-i-n cells, respectively, should be high enough to collect the maximum number of photo-generated carriers (electron-hole) and hence to enhance the efficiencies of the solar cells. But simultaneously the recombination rate increases with increasing the **E**, resulting in a reduction in the efficiency. Thus, there must be restriction to choose the effective doping concentration and thickness of p-layer so that the ultimate enhancement of efficiency occurs by compromising between the recombination rate and the electric field inside the cell.

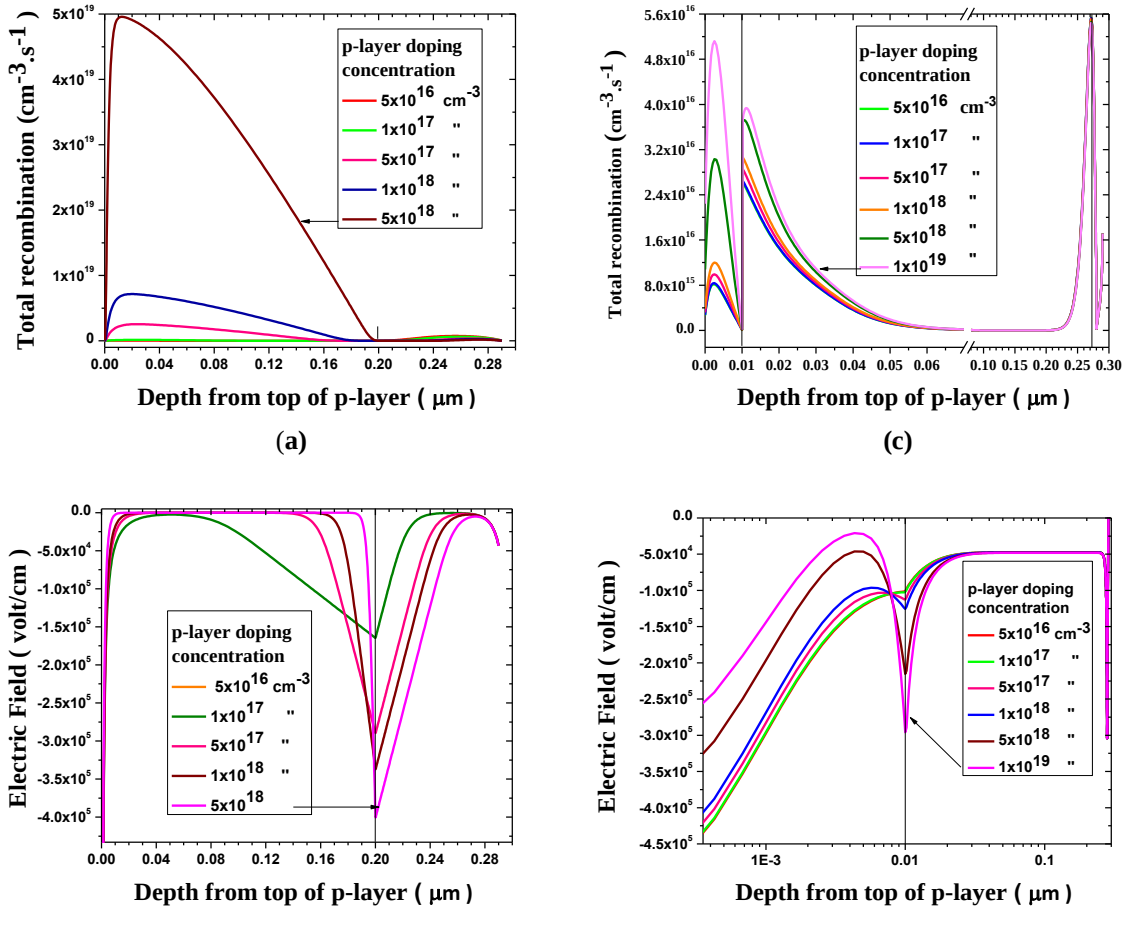

Figure 2: Recombination rate and electric field distribution of the [(**a**), (**b**)] p-n and [(**c**), (**d**)] p-i-n GaInN solar cell devices for different acceptor concentrations.

Fig. 2 shows the electric field distribution and recombination rate through the p-n (figs. a, b) and p-i-n (figs. c, d) cells as a function of p-layer doping concentration. It is observed from the figures that for high doping concentration of p-layer such as 5×10^{18} cm^{-3} for p-n cell and 1×10^{19} cm^{-3} for p-i-n cell, the magnitude of electric field intensity is highest at near the p/n (fig. 2b) and p/i (fig. 2d) interfaces that results more photo-generated carriers collection by ITO layer due to more absorption of photons as increase of conductivity in the layer, but simultaneously they also have highest recombination rates in p-layer. Ultimately, the optimum efficiency is obtained for p-layer doping concentration of 5×10^{17} cm^{-3} for p-n cell (fig. 4a)and 5×10^{16} cm^{-3} (fig. 4b) for p-i-n cell using n-layer doping concentration fixed at 5×10^{17} cm^{-3}, for good ohmic front and back contacts (high surface recombination velocity $\sim1\times10^{7}$ cm/s) due to less passivated surface of the solar cells by compromising between the recombination rate and the electric field.

The electric field distribution, photo-generation and recombination rate through the p-n and p-i-n cells as a function of p-layer thickness are shown in figs.3a, b, c and figs. 3d, e, f, respectively. These figures show that the cells with thinner p-layer has lower recombination rate in that layer and higher in n-layer with respect to other thick layers and same magnitude electric field in p/n interface of p-n cell results in higher current density and hence in the efficiency (fig. 7a) for 200 nm thickness of p-layer. Similarly, the fig. 3e for p-i-n cell shows the lower recombination rate and hence higher efficiency (fig. 7b) for thinner (10 nm) p-layer.

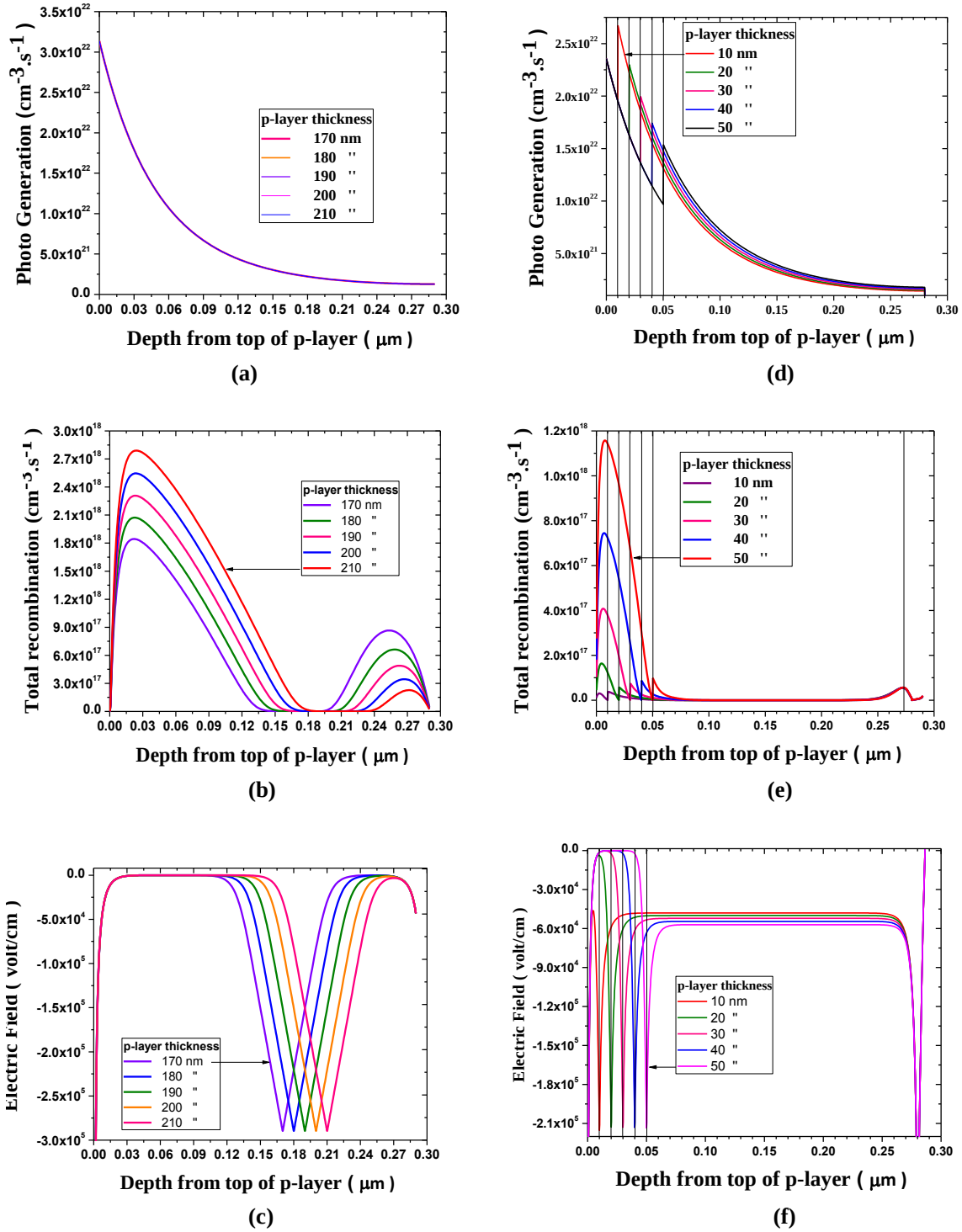

Figure 3: Photo-generation rate, recombination rate and electric field distribution of the [(**a**), **(b), (c**)] p-n and [(**d**), (**e**)**, (f**)] p-i-n GaInN solar cell devices for different thickness of p-layer.

Also the photo-generation decreases in general fashion as increase of device thickness which is clearly shown in figs 3a & 3d. The photo-generated carriers in p/i interface (fig. 3d) of p-i-n cell decreases with increase of p-layer thickness where for p-n cell at the p/n interface (fig. 3a) it remains constant, independent of top (p) layer thickness.

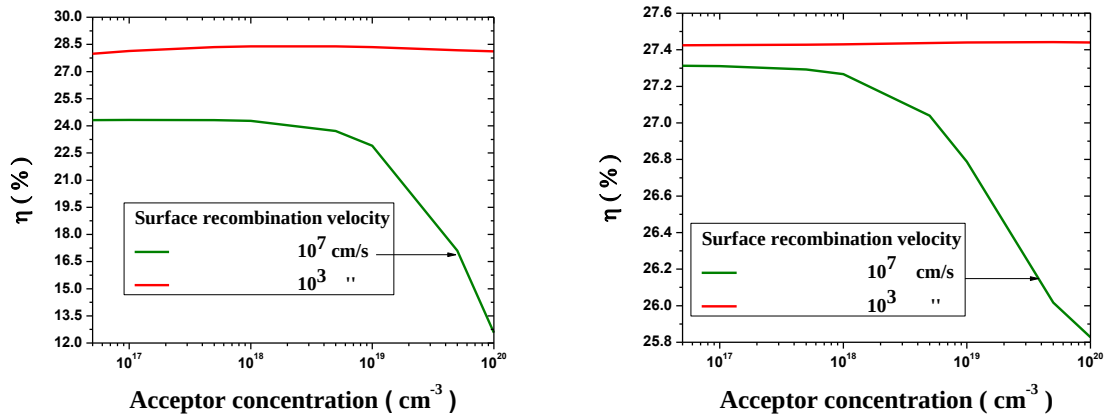

Figure 4: Variation of efficiency (η) as a function of acceptor concentration for **(a)** p-n and **(b)** p-i-n cells.

The variation of efficiency (η) with acceptor concentration (N_A) as parameter of surface recombination velocity is shown in figs. 4a and 4b for p-n and p-i-n cells, respectively. The curves show that the efficiency remains almost constant throughout the entire range of doping concentration from 5×10^{16} to $1 \times 10^{20} cm^{-3}$ for low surface recombination due to good surface passivation and for high surface recombination due to less passivated surface, the same (η) remains nearly constant for N_A up to the order of $1 \times 10^{18} cm^{-3}$ and then decreases sharply for p-n cell than p-i-n cell. Also the optimized efficiency of p-i-n cell is higher about 3% for N_A of $5 \times 10^{16} cm^{-3}$ than p-n cell for N_A of $5 \times 10^{17} cm^{-3}$ at high surface recombination.

J-V characteristics of the cells

Fig. 5 shows the current density–voltage ((J-V) characteristics as parameter of p-layer doping concentration (N_A) of p-n and p-i-n GaInN cells for total device thickness of 290 nm. It is observed from the figs. that the J_{SC} of p-n cell decreases prominently with minute decrease of V_{oc} with increase of N_A and the optimum efficiency is obtained for $5 \times 10^{17} \text{cm}^{-3}$ doping concentration of p-layer. But for p-i-n cell the same (J_{SC}) is changed slightly with constant higher V_{oc} than p-n cell which is common property of higher band gap material used in p-layer of the cell. The V_{oc} of p-i-n cell is independent of p-layer doping concentration reveals too small decrease of efficiency (fig. 4b) due to very small decrease of J_{SC} (fig. 5b) for low acceptor concentrations below $1 \times 10^{18} \text{cm}^{-3}$ for high surface recombination velocity.

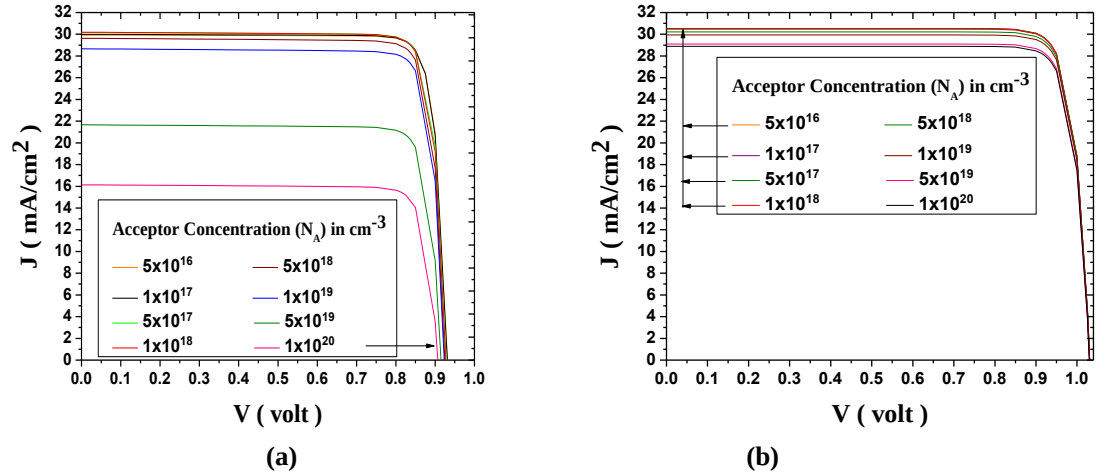

Figure 5: J-V characteristics as parameter of p-layer doping concentration of **(a)** p-n cell and **(b)** p-i-n cell for surface recombination velocity 10^7cm/s.

Effect of indium concentration on performance of $Ga_{1-x}In_xN$ solar cell

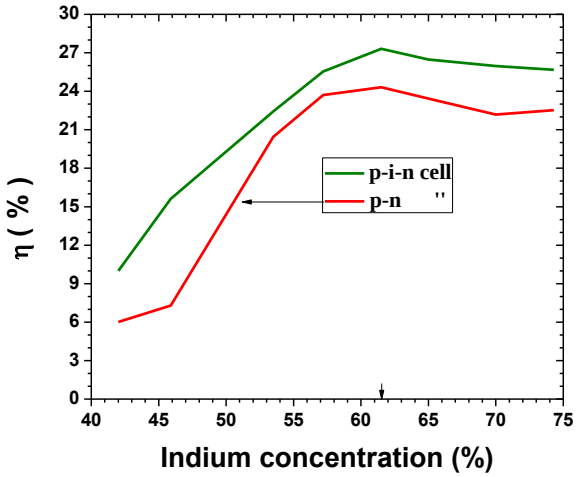

Figure 6: Variation of η as a function of indium concentration for surface recombination velocity 10^7cm/s.

The comparison of efficiency as a function of indium concentration from 42 to 74.3 % for high surface recombination is shown in fig. 6. The curves for both p-n and p-i-n cells show the optimum efficiency at 61.5% of In concentration. It is also observed from the curves that the efficiency of p-i-n cell dominates with respect to p-n cell through whole range of In concentration and the dominating optimum efficiency is 27.314 %.

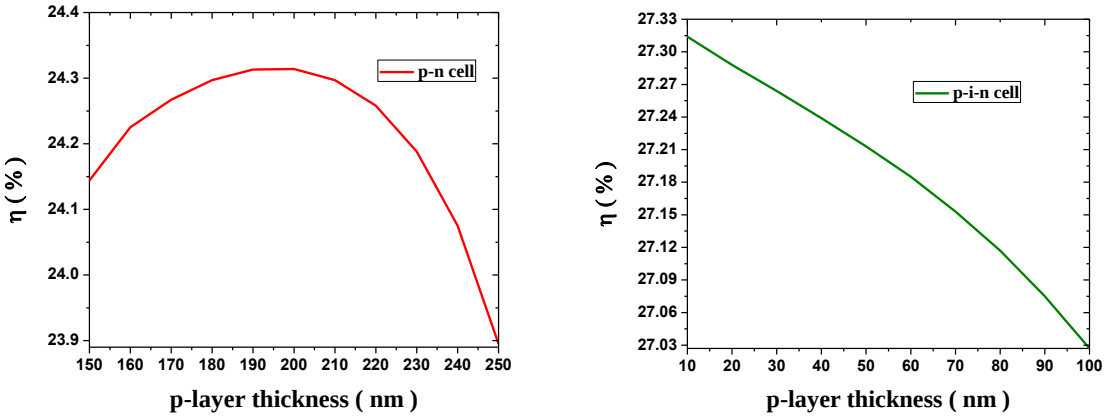

Figure 7: Variation of η as a function of p-layer thickness for (a) p-n cell and (b) p-i-n cell of total device thickness 290 nm.

Fig. 7 shows the variation of efficiency with p-layer thickness for p-n and p-i-n solar cells remaining other parameters are the same as specified in Table 2 for high surface recombination velocity. The thickness of the p-layer is varied from 150 to 250 nm for p-n cell and 10 to 100 nm for p-i-n cell. The optimum efficiency for first cell is obtained 24.314% for 200 nm thickness and 27.314% for second cell with p-layer thickness of 10 nm. It is also noted that for the expense of only about 0.29% efficiency of p-i-n cell, there is a freedom to choose the p-layer thickness up to 100 nm that can be used instead of 10 nm so that the total device thickness (290 nm) remains constant. But, in general, the thickness of p-layer should be taken small so that maximum amount of incident light will reach into i-layer.

Efficiency as a function of i-layer thickness

In GaInN thin film p-i-n solar cell, a thick i-layer can absorb more light than thin layer to generate electron-hole pairs but it degrades the drift electric field for carrier transport. Thus thickness of i-layer is a key parameter that can limit the performance of thin film solar cells. The comparison of efficiency as a function of i-layer thickness for the p-i-n cell is shown in fig. 8 for two surface recombination velocities. The less passivated surface (10^7cm/s) where the surface recombination deteriorates the cell performances, there the efficiency increases with i-layer thickness which is optimum at 270 nm, and then it decreases due to degradation of drift

electric field. Similarly, for low surface recombination (10^3cm/s) due to good surface passivation where the cell performances are enhanced with respect to first one, there also efficiency (optimum 27.426%) decreases after the same thickness of i-layer due to decrease of drift velocity of carriers and for bulk recombination within the absorbing (i) layer for such higher thickness. Also the two curves are almost overlapped at higher thickness by showing the efficiency differences only 0.016% and 0.11%, respectively, for 3980 and 270 nm thicknesses of i-layer and 1.08% for well separated curves for lower thickness at 10 nm. Therefore, i-layer and good surface passivation are equally important to obtain the best performances of p-i-n thin film solar cell at or below 270 nm thickness.

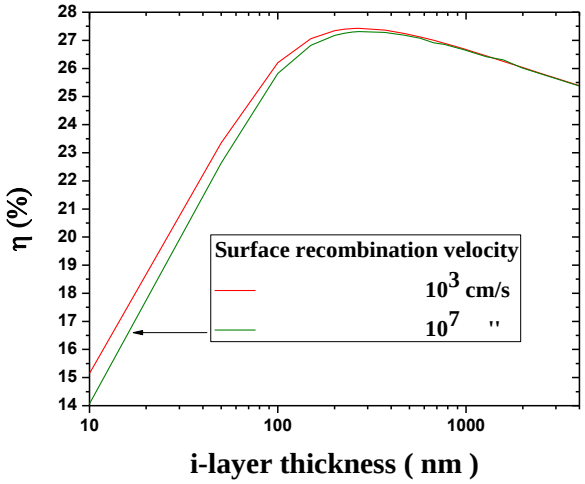

Figure 8: Variation of η as a function of i-layer thickness of p-i-n solar cell.

VI. Conclusion

The optimum performance of the p-n and p-i-n solar cells are simulated by AMPS-1D to study the dependence on p-layer properties such as doping concentration, thickness, surface recombination and i-layer properties such as thickness of absorbing layer. The flexibilities to desire the p-layer thickness and doping concentration for p-i-n cell are better than the p-n cell with no significant change of efficiency in spite of less passivated p-layer surface. Also the best performance is obtained for p-layer doping concentration of $5 \times 10^{16}\text{cm}^{-3}$ for p-i-n solar cell which is one tenth of p-layer doping concentration of p-n cell with indium concentration of 53.5%.

Acknowledgement

The author acknowledges the use of AMPS-1D program that was developed by Dr. Fonash's group at Pennsylvania State University.

References

[1]. Jani, O., Ferguson, I., Honsberg, C., Kurtz, S., "Design and characterization of GaN/InGaN solar cells," Appl. Phys.Lett., 91, 2007, 132117.
[2]. Xiaobin Zhang et al, "Simulation of In0.65Ga0.35 N single-junction solar cell" J. Phys. D: Appl. Phys., 40, 2007, 7335–7338.
[3]. Hamzaoui, H., Bouazzi, A. S. and Rezig, B., "Theoretical possibilities of InxGa1-xN tandem PV structures," Sol. Energy Mater. Sol. Cells 87, 2005, 595-603.
[4]. Tae Hoon Seo et al., "Improved photovoltaic effects in InGaN-based multiple quantum well solar cell with graphene on indium tin oxide nanodot nodes for transparent and current spreading electrode" Appl. Phys. Lett., 102, 2013, 031116.
[5]. Fonash, S. et al., http://www.cneu.psu.edu/amps/.
[6]. Wu, J., Walukiewicz, W., Yu, K. M., Ager III, J. W., Haller, E. E., Lu, H., Schaff, W. J., Saito, Y. and Nanishi, Y., "Unusual properties of the fundamental band gap of InN," Appl. Phys. Lett., 80, 2002, 3967-3969.
[7]. Levinshtein, M. E., Rumyantsev, S. L. and Shur, M. S., Properties of Advanced Semiconductor Materials, (Wiley, Chichester, UK, 2001, 1–90).
[8]. Mnatsakanov, T. T., Levinshtein, M. E., Pomortseva, L. I.,Yurkov, S. N., Simin, G. S. and Asif Khan, M., "Carrier mobility model for GaN" Solid-State Electron. 47, 2003, 111-115.